

Water Hyacinth Plant Fibre Characterization

Awari A. Ishaya¹, Augustine U. Elinwa^{2*}, Isah Y. Mohammed³

¹Building and Construction Dept., University of Jos. Plateau State, Nigeria.

²Civil Engineering Dept. Abubakar Tafawa Balewa University, Bauchi, Bauchi State, Nigeria*

³Chemical Engineering Dept. Abubakar Tafawa Balewa University, Bauchi, Bauchi State, Nigeria

*Corresponding Author

DOI: <https://doi.org/10.51244/IJRSI.2024.1109098>

Received: 01 September 2024; Accepted: 11 September 2024; Published: 18 October 2024

ABSTRACT

This work is on the specie of the water hyacinth (WH) in the Northern part of Nigeria taken from the lake in Jalingo in the Sahel region of the country. The basic characteristics of the fibres are studied for use in concrete and other allied construction works. They are subjected to physical and chemical tests for the determination of their properties. X-ray diffraction and scanning electron microscopy are applied to study the crystalline phases and mineral oxides, and the morphology and structural characteristics of the WHFs. The TGA/DTA and FTIR methods of analysis are applied to the WHFs to identify and investigate the thermal stability and percentage of weight loss on temperature, and the SEM for the morphology and structural characteristics of the WH fibre. The results show that the presence of peaks on the spectra of the cellulose samples corresponds to bands of microcrystalline cellulose. The WH plant fibre has a moisture content of approximately 13.7 %, density of 666.7 kg/m³, specific gravity of 0.86, and water absorption of 1067 %, and the cellulose, hemicellulose, lignin are 14.1, 21.5, 7.1 %, respectively. The WH fibre has a tensile strength of 0.12 MPa, Young Modulus of 7.7 GPa, elongation of 4.8 %, tensile extension at break of 2.89 mm, and energy at break of 1.04 x 10⁻³ J. The XRD diffractogram characterization shows that the WH fibre is crystalline in nature, while the FT-IR shows the functional group change of each treatment respectively. The thermal decomposition process of the WH fibre resulted in similar TG and DTG curves due to being lignin cellulosic material. These curves showed a distinct DTG peak (cellulose) and a high-temperature tail (lignin). The morphology of WH fibre shows a well-shaped fibril with a rigid lignin structure coated surface with the capacity to hold the liquid contents with good absorbency. The chemical compound compositions of the WH fibre contains Ca, K, Cl, C, Al, Si, Fe, S, Y, Ti, P, Mg, Na, and N.

Keywords: Water Hyacinth fibre; Physical and Chemical Characterization; XRD and SEM; TGA/DTA and FTIR analysis.

INTRODUCTION

Sustainability in the construction and engineering industry is moving away from the finite materials to infinite materials. Recent research awareness focuses on the use of renewable materials. This has caused a shift from the classical to the environmentally friendly materials. The utilization of renewable materials in industry as a major strategic approach of 21st century is mainly focused on the development of bio-based building materials [1]. In this class of organic materials is the Water hyacinth plant fibre. It is one of the most pervasive aquatic weeds that is very adaptable to the environment. Water hyacinth, a renewable material, has become an interesting study area. It is considered as engine for sustainability drive because it is abundant and cheap in Nigeria. However, lignocellulosic fibres have several disadvantages and contributes to its inefficient use in the construction sector. This, however, has been attributed to the lack of a complete understanding of

the anatomy, structure, and chemical composition of WHF, the hydrophilic nature of the lignocellulosic fibres which can contribute to fast humidity absorption, leading to a consequent loss of dimensional stability of the manufactured part [2 and 3], Another disadvantage is from the age of the plant and its harvesting time variability of their properties, ranging from the age of the plant and its harvesting time, to soil fertility and weather variations. However, these setbacks can be addressed through technology that will improve and upgrade the characteristics of the material. Therefore, in-depth characterization of WH as a material is necessary to find efficient uses for WH in the construction industry. Biswas et. al took a comparative study of the various pre-treatment techniques for water hyacinth cellulose. The trust was improving the quality of the fibre material using various levels and types of treatments [4, 1].

Plant fibres are classified as lignocellulosic materials. They are composed of three main components: namely, cellulose, hemicellulose, and lignin, with cellulose as the main chemical component, with differing amounts of hemicellulose and lignin [5], Cellulose is mainly of hollow cellular fibrils entrenched together by lignin and hemicellulose matrix [6]. This determines the tensile strength of the material. The lignin is responsible for resistance against biodegradation and hemicellulose binds the cellulose polymers, providing secondary strength, and absorbs moisture [7, 8, 9]. The cellulose content in water hyacinth is high and good material for construction because of the characteristics of having a very strong wall, and one of the most important polysaccharides in the plant cell wall. Therefore, understanding the structure-function relationship of the WHF is of critical importance for successful incorporation in concrete production, and for this to actualize, the applications and use of modern analytical tools becomes necessary to unlock detailed information on their characteristics and composition. The present study focusses on further characterization of water hyacinth (WH) plant material using available technology such as the x-ray diffraction analysis (XRD), scanning electron microscopy (SEM), fourier transform infrared spectroscopy (FTIR), and the thermogravimetric analysis (TGA), to study the physio-chemical composition, the morphology and structural characteristics of the material, Thus, this is important due to the nature of the WH plant and the inherent variabilities arising from the environmental impact, and where the WH plant is grown.

MATERIALS AND METHODS

The water hyacinth (WH) used for this investigation is harvested from a lake in Jalingo, Taraba State, Nigeria, measuring up to 40 cm. Water hyacinth is a rhizomatous plant with long, pendant and adventitious roots. The stem of the WH is cleaned, and the roots and leaves were cut off using a sharp knife. The bundles of the stem of the WH are tied and submerged in water for [?] before the extraction of the fibres. The water hyacinth fibres are subsequently spread out in loose bunches for 48hr to dry at room temperature. This procedure ensures even drying, reduction of the effect of clumping, and when dried, allowed for easy separation without damage. Drying is necessary to remove fibre moisture and prevent over-fermentation. These processes are shown in Plate 1(a to d).



a- Water Hyacinth Plant

b- Water Hyacinth Plant Stalk



c- Water Hyacinth Fibre Retting

d- Extracted Water Hyacinth Fibre

Plate 1: Water Hyacinth Harvesting and Fibre Extraction

Physical Characterization of the WHFs

The physical characterization in this process involves the determination of; i- the moisture content, ii- density, iii- diameter, iv- specific gravity, and v- water absorption of the WHFs.

i. Moisture content

The moisture content of the water hyacinth fibre is carried out in accordance with ASTM D2495 [10], and is carried out using 5g of the WHF at a standard atmosphere of 20°C and 65 % RH. The WHFs were placed in an air oven at a constant temperature of 105°C at 15min intervals until the moisture content change attains a value less than 0.1 %. The moisture content is calculated as:

$$\text{Moisture (\% M)} = \frac{w_2 - w_1}{w_1} \times 100 \dots\dots 3$$

Where.

w_1 = the wt. before oven-dried

w_2 = the wt. after oven-dried

ii. Density of Water Hyacinth Fibre

The bulk density of the WHF was determined using mass volume ratio relationships. The true density was determined using the toluene (C7H8) displacement method [11]. This is given as:

$$\rho = \frac{w_2 - w_1}{v} \text{ kgm}^{-3} \dots\dots 4$$

Where.

ρ = Density of the WHF sample (kg/m³)

w_2 = Weight of the container and sample (kg)

w_1 = Weight of the container (kg)

v = volume of the container (m³)

iii. Diameter of WHF

The diameter of the WHF is determined using a computer-controlled Carl Zeiss SEM machine EVO LS 10 model, and the measurements are taken on three (3) locations of each 40 mm gauge length of fibre, at the middle and at the two (2) ends shown in Figure 1 and the average is used as the diameter of the WHF.

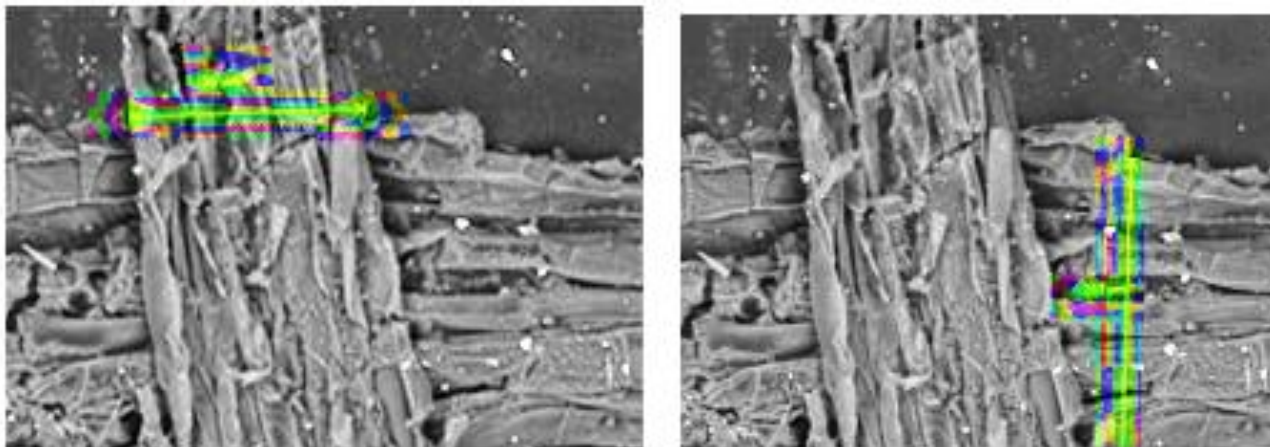


Figure 1: Water Hyacinth Fibre Diameter Measurement

iv. Specific Gravity of Water Hyacinth Fibre

The specific gravity of the WHF is determined using a pycnometer and a digital weighing machine, The fibre material is dried in an oven for a period of 24 h, at a temperature of 50°C. The specific gravity bottle/pycnometer is also completely dried and weighed with its cap tightly screwed as, M_1 , and the position of the screwed cap marked. This is to maintain the uniformity in screwing the cap. The cap of the bottle is unscrewed and the dried fibre from the oven placed in it. This is weighed again, and the weight taken as M_2 . The bottle is now filled with the kerosene to the specified mark and weighed as, M_3 , and the excess kerosene mopped with a cloth. The specific gravity bottle is again filled with kerosene but without the fibre, and marked as, M_4 . The specific gravity is then determined as:

$$SG = \frac{M_s}{M_s + M_4 - M_3} \dots 5$$

Where;

SG = Specific gravity

M_s = the mass of fibre ($M_2 - M_1$) (g)

M_1 = Mass of empty pycnometer (g)

M_2 = Mass of pycnometer + dry fibre (g)

M_3 = Mass of pycnometer + dry fibre + kerosene (g)

M_4 = Mass of pycnometer + kerosene (g)

v. Water absorption of Water Hyacinth Fibre

The water absorption of the WHF is tested in conformity to ASTM D 570-98 Standard [12] using the dry fibre samples of 10g. These are cut into lengths ranging between 40-50 mm and immersed in water for 24h, and the excess water removed with a dippier, and labelled as w_1 . The saturated fibre samples are weighed

and dried in an oven for 24h. This is taken as w_2 . The difference in weight is taken as the water absorption. The moisture content, diameter, density, specific gravity, and water absorption of the WHF are shown in Table 2

Table 2 Physical Properties of WHF

Parameter	Value
Moisture (%)	13.7
Diameter (μm)	229.5
Density (kgm^{-3})	666.7
Specific Gravity	0.86
Water Absorption (%)	1067

Chemical Composition of WHF

The chemical composition of the untreated water hyacinth fibers is determined using the Technical Association of the Pulp and Paper Industries (TAPPI) standard and other methods for different components, namely T 203 cm-99 (α -cellulose) and T 222 om-06 (lignin) [13]. The holocellulose is recorded and determined following the method described by Wise et al. [14], and the hemicellulose fraction is calculated as the difference between the holocellulose and α -cellulose contents. The percentage contents of extractive, α -cellulose, hemicellulose, and lignin are determined, and the average and standard deviation values were based on the sample report

$$\%H = \%h - \%c \quad \dots \quad 2$$

Where.

$$H = \text{Hemicellulose (\%)}$$

$$h = \text{holocellulose (\%)}$$

$$c = \text{Cellulose (\%)}$$

Crude Protein, Crude Ffibre and Ash Content of WHF

The crude protein and crude fibre of WH are determined after chemical digestion and solubilization of other materials present in the sample, following the Association of Official Analytical Chemists (AOAC) methods specification 950.46 AOAC [13]. Approximately 2g of the sample (w) was extracted by boiling in 200 mL of 1.25 % H_2SO_4 for 30 min under a reflux condenser. After various processes of treatments, the residue was dried in an oven at $105^\circ C$ in a porcelain dish to a constant weight (w_1). Incineration was done in a muffle furnace at $550^\circ C$ for 3 h, the dish was then cooled in a desiccator, and the final weight (w_2) was taken. The crude fibre is calculated as:

$$Cf (\%) = \frac{w_2 - w_1}{w_1} \times 100 \quad \dots \quad (1)$$

Where:

$$Cf = \text{Crude fibre (\%)}$$

$$W_1 = \text{Initial weight}$$

$$W_2 = \text{Final weight}$$

To determine the ash content in the water hyacinth 5 g of air-dried sample is put in the preconditioned crucible and the sample first charred by flame to eliminate organic material before incineration at 550°C in a muffle furnace to the point of white ash. The residue is cooled in a desiccator and the weight taken as the ash content. The percentage content of total carbohydrate in the WH is calculated by subtracting the sum of moisture, protein, fat, ash and crude fibre percentages from 100 [13]. The results of the above analysis are shown in Table 3, while Table 4 is a comparison between the present and past researchers.

Table 3: Chemical Characteristics of WHF

<i>Fibre Characteristics</i>	<i>Value (%)</i>
<i>Cellulose</i>	14.05
<i>Hemicellulose</i>	21.49
<i>Lignin</i>	7.08
<i>Ash Content</i>	10.87
<i>Crude Protein</i>	3.94
<i>Crude Fibre</i>	29.08

Table 4: Comparisons: Present and Past Researchers- Cellulose, Hemicellulose, and Lignin

<i>Reference</i>	<i>Cellulose (%)</i>	<i>Hemicellulose (%)</i>	<i>Lignin (%)</i>
<i>Opeyemi I et al [15]</i>	29.33	28.35	18.36
<i>R.Kumar et al [16]</i>	18.40	49.2	3.55
<i>B. Sornvornweat et al [17]</i>	19.20	32.69	4.37
<i>J.G. Realeset et al [18]</i>	31.67	27.33	3.93
<i>M. Narra et al. [19]</i>	38.01	24.00	9.50
<i>V.B. Barua and A.S. Kalamdhad [20]</i>	32.84	24.70	8.10
<i>S. Rezania et al [21]</i>	16.40	32.00	5.70
<i>S. Kumari and D. Dan [22]</i>	24.80	30.00	5.60
<i>Mochamad et al [23]</i>	43.0	29.0	7
<i>Auangfa et al [24]</i>	22.05	32.60	4.53
<i>Biswamth Biwas et al [25]</i>	20.5	40.1	13.9
<i>M. Bhuvareshwavi and K. Sangeetha [26]</i>	63.75	12.33	20.67
<i>WJJ Thangiah et al [27]</i>	65.38	32.45	3.14
<i>A. Arivendan et al [28]</i>	65.4	12.8	7.2
<i>F Filrya [29]</i>	46.15	14.46	23.07

MECHANICAL CHARACTERIZATION OF WATER HYACINTH FIBRE

The elemental composition of the untreated water hyacinth fibre plant is analyzed using the Thermo-Fisher Scientific elemental and radiation detection solution. This combines sophisticated technology including X-ray Fluorescence Spectroscopy (XRF), Laser Induced Breakdown Spectroscopy (LIBS), and radiation detection to achieve the desired results (Plate 1).



Plate 1: Thermo-Fisher Scientific Equipment (XRF)

The minerals in the WHF are estimated using the Atomic Absorption Spectrometry (AAS) described in AOAC, 1990 [30], and shown in Table 5 and Figure 2.

Table 5: Mineral Composition of the WHF

Element (Oxide)	Mineral	
	Element (%)	Oxide (%)
Ca (CaO)	1.87	2.620
Na (Na ₂ O)	0.16	0.220
K (K ₂ O)	0.23	0.277
Mg (MgO)	0.02	0.235
Cu (CuO)	0.00	0.001
Zn (ZnO)	0.00	0.004
Fe (Fe ₂ O ₃)	0.43	0.062
Ni (NiO)	0.05	0.062
Al (Al ₂ O ₃)	0.03	0.062
S	0.13	0.133
Mn (MnO)	0.14	0.021
Rb (Rb ₂ O)	0.00	0.0002
Sr (SrO)	0.00	0.003
Br (Br)	[0.0001]	[0.0001]
Cl	0.177	0.177
Cr (Cr ₂ O ₃)	0.000	0.000
V (V ₂ O ₅)	0.000	0.000

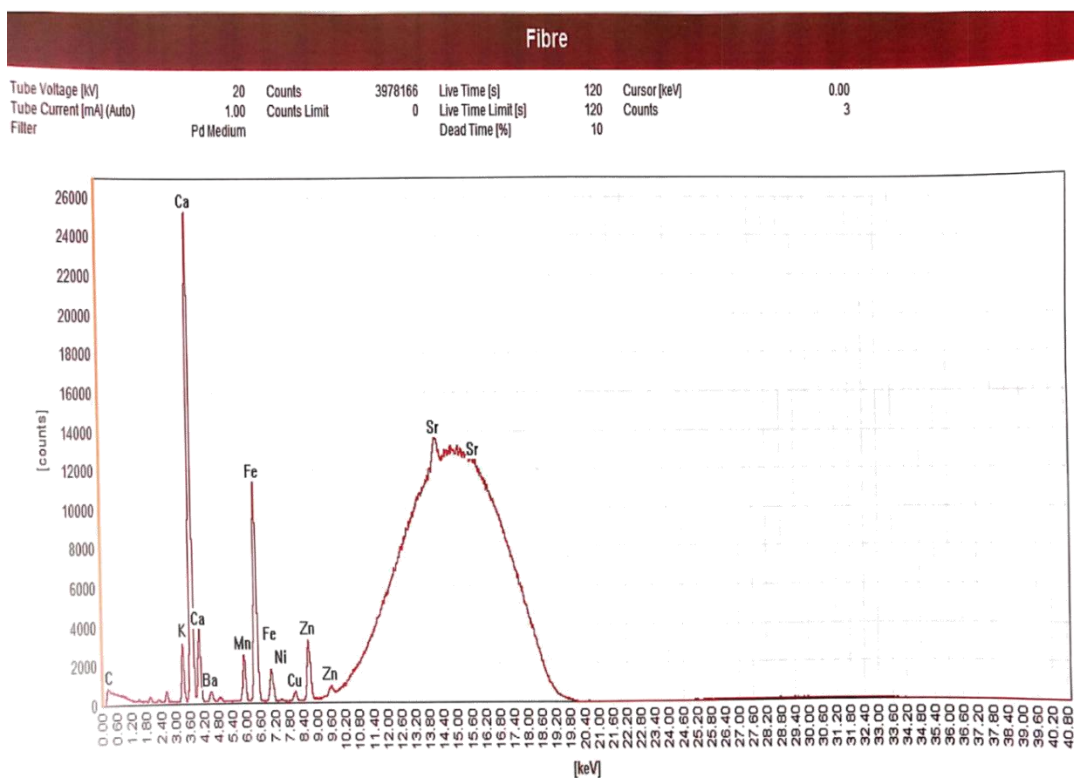


Figure 2: X-Ray Spectrograph of WHF

Fibre Tensile Strength of WHF

The mechanical properties of the water hyacinth fibre were prepared and tested according to ASTM D 3822M-14 [31], for testing the tensile properties of single natural and man-made fibres. These fibres were tested in the materials laboratory of Energy Research Development, Obafemi Awolowo University (OAU), Ife, Ogun State, Nigeria. They were tested using a computer-controlled 100 kN capacity Universal Instron 3369 testing machine (Plate 2) at a constant crosshead speed of 1 mm/min at room temperature. The load was applied at a constant rate and recorded until failure was attained. A gauge length of 60 mm was used, and three (3) fibre samples were tested for the various mechanical properties, and the average recorded. The results of mechanical fibre strength are shown in Figure 3 and Table 6.



Plate 2: Tensile Strength of UTWHF Using Universal Instron Testing Machine

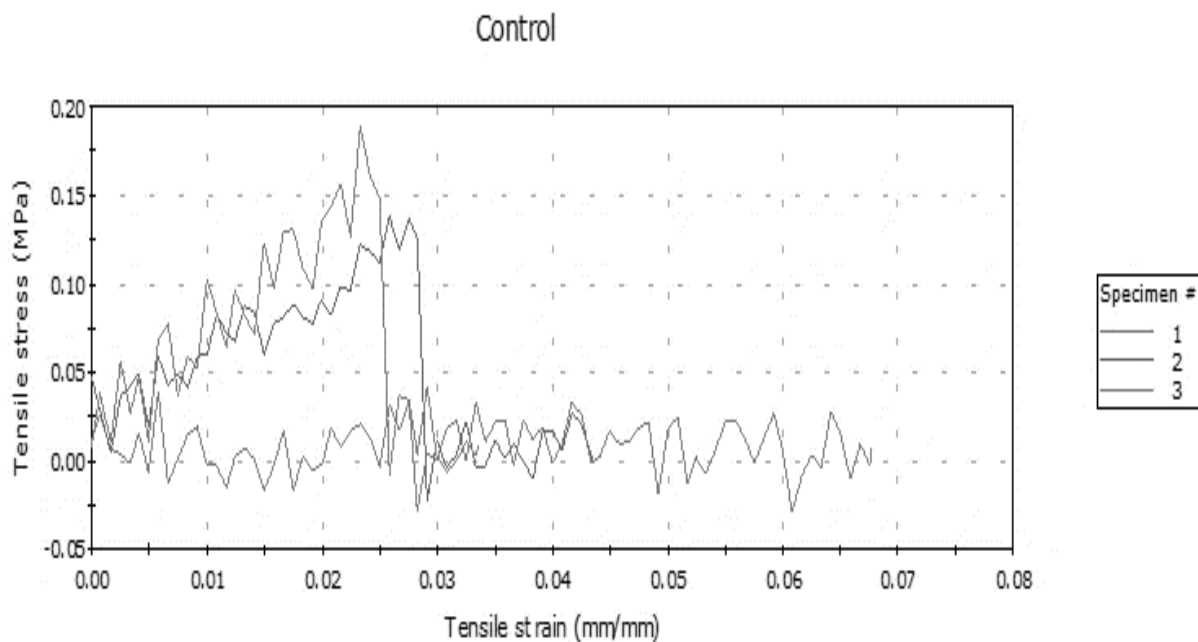


Figure 3: Stress-Strain of Water Hyacinth Fibre

Table 6: Mechanical Characteristics of WHF

Parameter	Fibre Specimen $\times 10^{-3}$			Mean $\times 10^{-3}$	Std. Dev $\times 10^{-3}$
	1	2	3		
Max Str. Stress (MPa)ax. Tensile	39.46	1381.27	189.47	122.35	76.24
Load at Max Tensile Stress (N)	394.63	1381.27	1894.72	1223.54	.762.38
Tensile Strain at Max Tensile Stress (mm/mm)	5.83	25.83	23.33	18.33	.1090
Energy at Max. Tensile stress (J)	0.03	1.08	1.17	0.76	0.63
Tensile stress at Break (Standard) (MPa)	8.13	2.94	7.56	621	2.84
Load at Break (Standard) (N)	81.31	29.44	75.56	62.11	28.43
Tensile strain at Break (Standard) (mm/mm)	67.70	43.33	33.57	48.20	17.58
Tensile extension at Break (Standard) (mm)	4.02.06	2599.94	2014.06	2892.02	1054.78
Energy at Break (Standard) (J)	0.32	1.36	1.43	1.04	0.62
Tensile stress at Yield (Zero Slope) (MPa)	-	-	-	-	-
Load at Yield (Zero Slope) (N)	-	-	-	-	-
Modulus (E-modulus) (gf/tex)	-	7832357.60	-	7832357.60	--
T-tensile stress at Yield (Offset 0 mm/mm) (MPa)	-	-	-	-	-

STRUCTURAL AND MORPHOLOGICAL CHARACTERISTICS OF UTWHF

Structural Characteristics of Untreated WHF

The structural characteristics of WHF are accessed using x-rays diffraction and thermogravimetric analysis methods.

X-ray characterization of UTWHF

The WH is one of potential natural fibre which contains cellulose considered as weeds plant in a water

environment, whose fibre material is not yet maximally used. The XRD characterization was in the form of powder using Rigaku Ultra III XRD Instrument (Plate 4), operated at room temperature using Cu-K α radiation at operating condition of V = 45 VA, I = 40 mA. The sample was analyzed using the reflection transmission spinner stage using the theta-theta settings. Two-theta at seventy-five degrees (75°) with a two-theta step of 0.026261 at 8.67 seconds per step. A programmable divergent slit with mask and a Gonio scan were used. The intensity of diffracted x-rays was continuously recorded as the sample and detector rotate through their respective angles. The x-ray detector offered in the diffractometer was used to scan the diffracted x-ray between 0° and 100° (2 θ). Results are commonly presented as peak positions at 2 θ and x-ray counts (intensity) in the form of a table or an x-y plot. The results are shown in Figure 4.

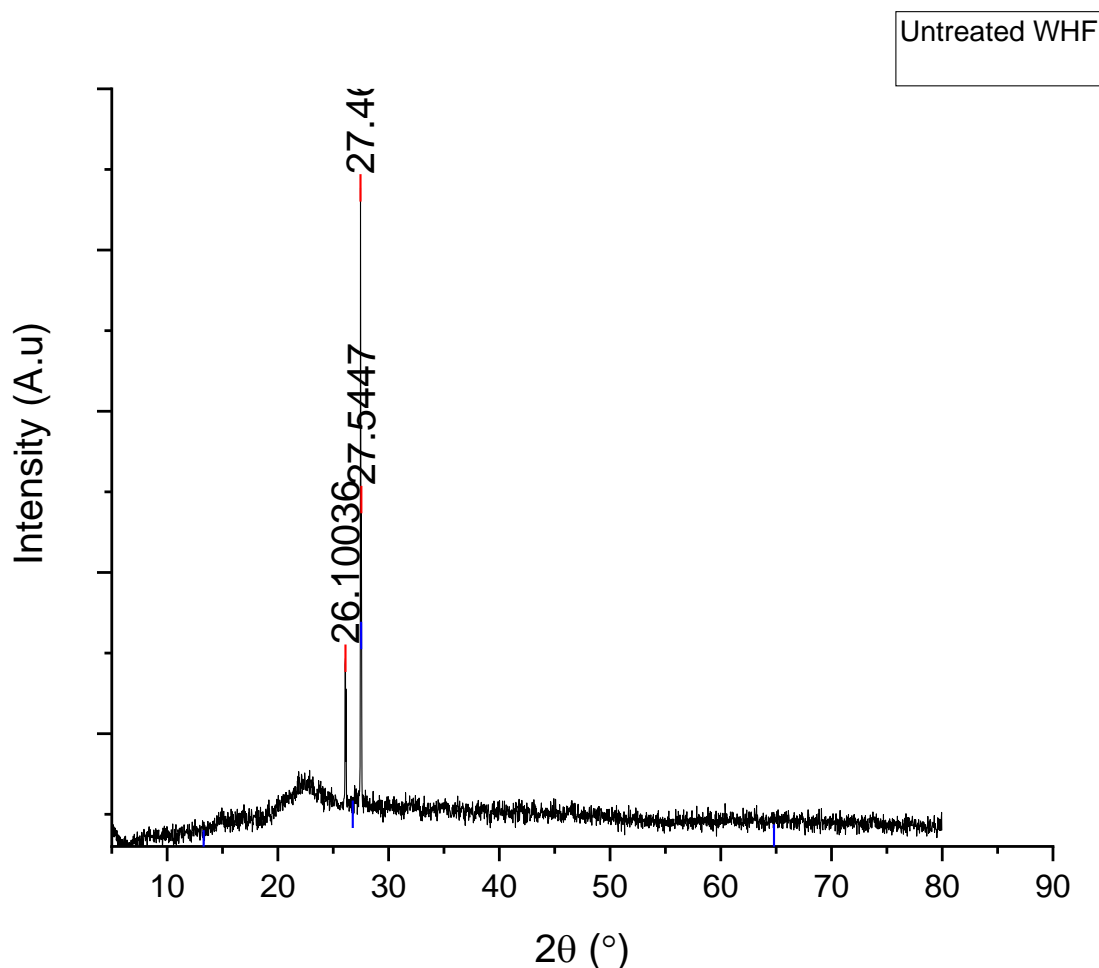


Figure 4 X-Ray Diffractogram of UTWH Fibre

Thermogravimetric analysis (TGA)

The thermogravimetric analysis is a thermal analysis technique used to measure changes in the weight loss (mass) of the sample subjected to a steady increase of temperature to quantify reactions involving gaseous emissions [32,33]. TGA involves heating a material to, and past its thermal degradation temperature at a controlled rate and monitoring mass loss during the heating process. The purpose for it is to measure its thermal stability using the thermal analyser Perkin Elmer TGA 4000 model. The change in weight loss is found by temperature and time. For the experiment, 11.874 mg of powdered WHF is placed over an aluminium crucible in a furnace with a controlled nitrogen environment with a flow rate of 20.0 mL/min. The rate of change of temperature is set at 10°C/min from room temperature to 700°C. The results are shown in Figure 5 (a-c).

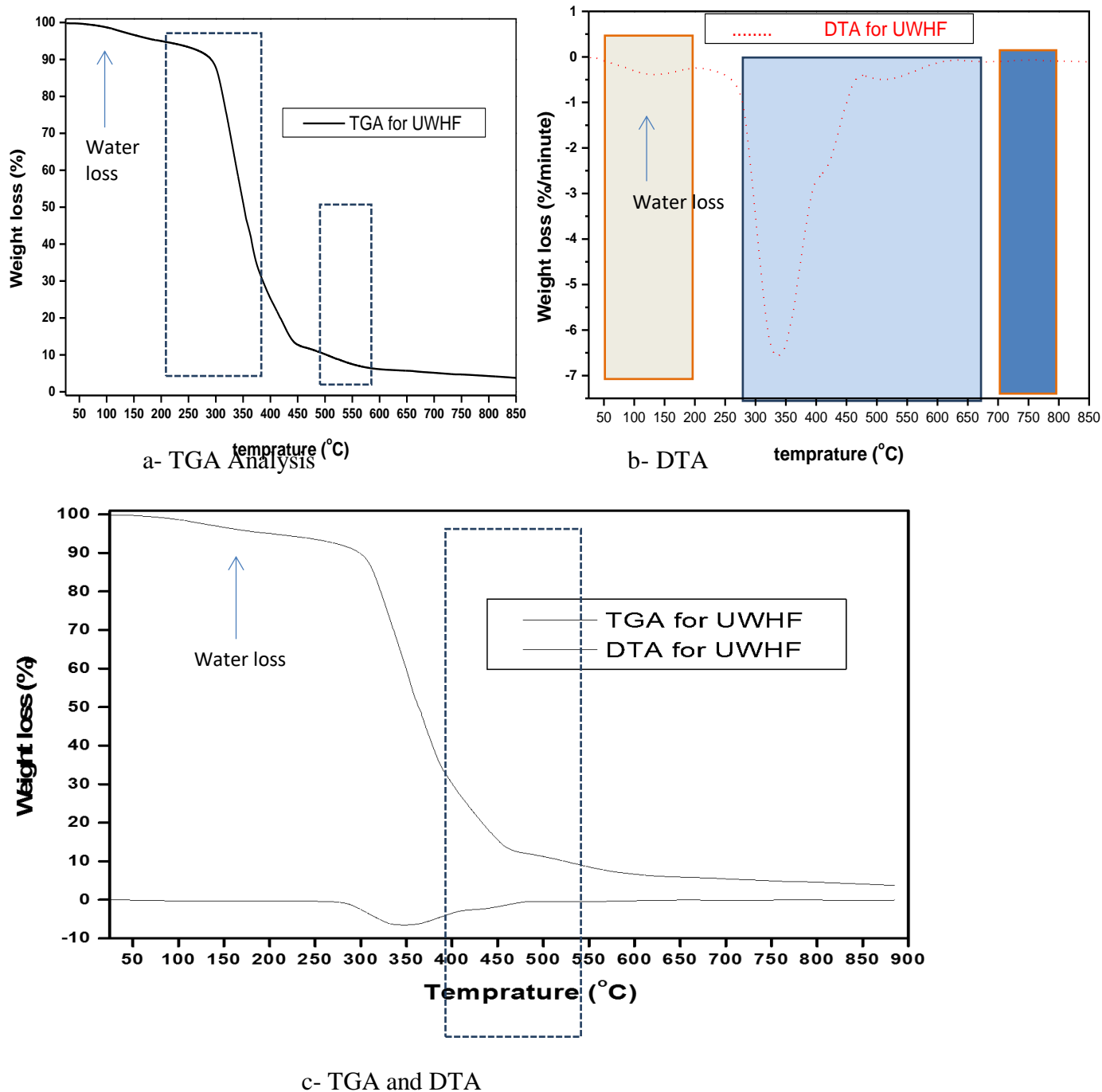


Figure 5: Thermographic Analysis

Morphology Study of WHF

Fibre surface plays a very important role in interfacial bonding between fibres and resin resulting in better mechanical properties. The surface morphological of the fibre is studied using the scanning electron microscopy (SEM) and digital image analysis, using an approximate quantity of fibre of 1 to 2 milligrams and 1 to 2 mm lengths. These are washed with dilute acetone and oven-dried at $80 \pm 5^\circ\text{C}$, and exposed to a plasma sputtering apparatus, coating the fibres with a thin gold layer in a vacuum atmosphere to improve the conductivity of the fibre. The coated surfaces are examined with PHENOM World Scanning Electron Microscope in a high-vacuum mode with a voltage of between 5 and 10 kV. The results of the micrograph and EDS-Spectrogramme are shown in Figure 6 and Table 7 while Table 10 is a comparison with the past researchers. Table 8 is a comparison of past work with the present.

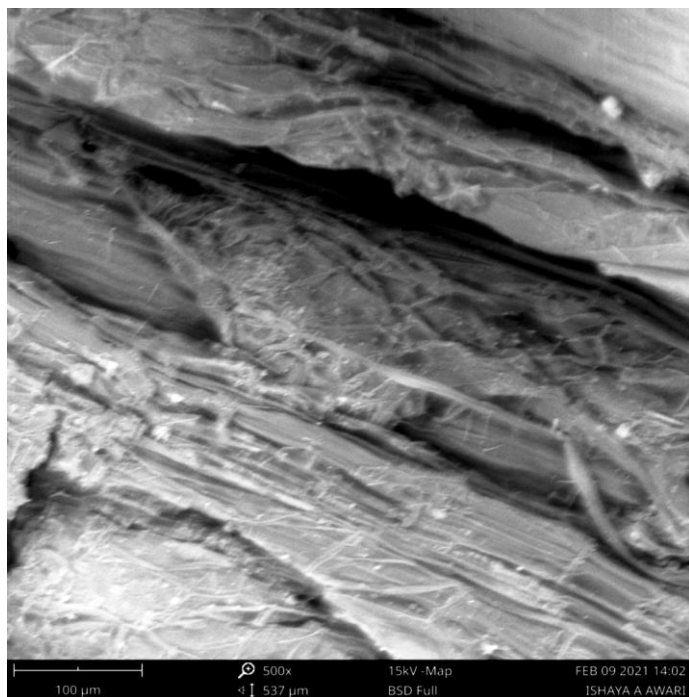


Figure 6: Morphology of the WHF

Table 7: EDS Spectrograph Characteristics

<i>Element</i>	<i>Symbol</i>	<i>Atomic Conc.</i>	<i>Weight Conc.</i>
<i>Calcium</i>	Ca	26.67	31.86
<i>Potassium</i>	K	22.32	26.02
<i>Chlorine</i>	Cl	16.58	17.53
<i>Carbon</i>	C	12.62	4.52
<i>Aluminum</i>	Al	4.45	3.58
<i>Silicon</i>	Si	4.09	3.42
<i>Iron</i>	Fe	1.64	2.73
<i>Sulphur</i>	S	1.97	1.88
<i>Yttrium</i>	Y	0.64	1.70
<i>Titanium</i>	Ti	1.05	1.51
<i>Phosphorus</i>	P	1.54	1.42
<i>Magnesium</i>	Mg	1.95	1.41
<i>Sodium</i>	Na	2.01	1.38
<i>Nitrogen</i>	N	2.46	1.03
<i>Silver</i>	Ag	-	-
<i>Zinc</i>	Zn	-	-
<i>Oxygen</i>	O	-	-

Table 8: Comparison (Wt. %)- Past Researchers

<i>Element</i>	<i>TR [34] *</i>	<i>YL [34]*</i>	<i>[42]</i>
<i>Calcium (Ca)</i>	15.05	20.27	4.73
<i>Potassium (K)</i>	38.36	41.49	8.26
<i>Chlorine (Cl)</i>	19.43	21.47	5.58
<i>Carbon (C)</i>	-	-	14.4

Aluminum (Al)	0.82	0.27	2.32
Silicon (Si)	8.06	1.97	5.33
Iron (Fe)	0.26	0.20	4.71
Sulphur (S)	2.44	0.37	-
Y	-	-	-
Titanium (Ti)	-	-	0.27
Phosphorous (P)	5.12	4.64	-
Magnesium (Mg)	5.33	6.00	1.96
Sodium (Na)	4.43	2/01	0.58
Nitrogen (N)	-	-	-
Silver (Ag)	-	-	-
Zinc (Zn)	-	-	-
Oxygen (O)	-	-	49.5
Zircon (Zr)	-	-	2.24
Copper (Cu)	-	-	
Magnesium (Mn)	0.70	1.31	

FOURIER TRANSFORM INFRARED SPECTROSCOPY (FT-IR)

FT-IR spectroscopy is an established technique for quality control and can often serve as the first step in the material analysis process. It measures a sample’s absorbance of infrared light at various wavelengths to determine the material’s molecular composition and structure. Fourier transform infrared spectroscopy (FTIR) is one of the most commonly used methods for identifying different functional groups constituting a compound. It is a rapid and non-destructive technique and provides information about molecular fragments, the presence or absence of specific functional groups, and can give an even deeper insight into the fibers structure. FT-IR spectroscopy works to convert the raw data from the broad-band source to obtain the absorbance level at each wavelength. The FT-IR machine (SHIMADZU 8400S, Japan) (Plate 3), was used to investigate the changes in the functional group of the WHF surfaces. The WHF of approximately 1 ± 0.2 mg were crushed in a crucible and blended with 100 ± 10 mg of potassium bromide (KBr) to form pellets. These were scanned at the scan rate of 30 per min and a resolution of 8 per cm in the wave number regions of 650 to 4000 cm^{-1} at room temperature of 30°C and relative humidity of 65 % was in absorbance mode as a function of the wavelength for each sample. The results of the FT-IR are shown in Figure 7.

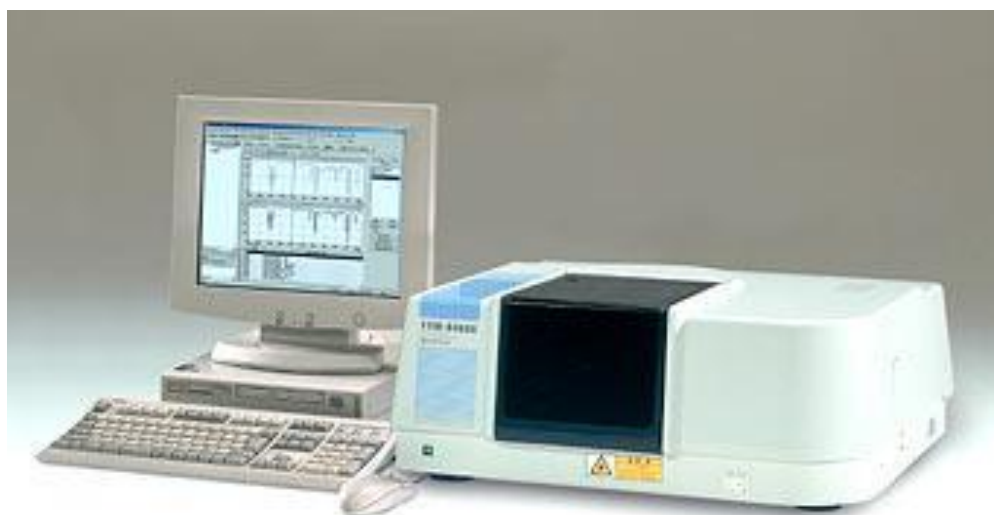


Plate 3: FT-IR Study of UTWHF Using SHIMADZU 8400S Equipment

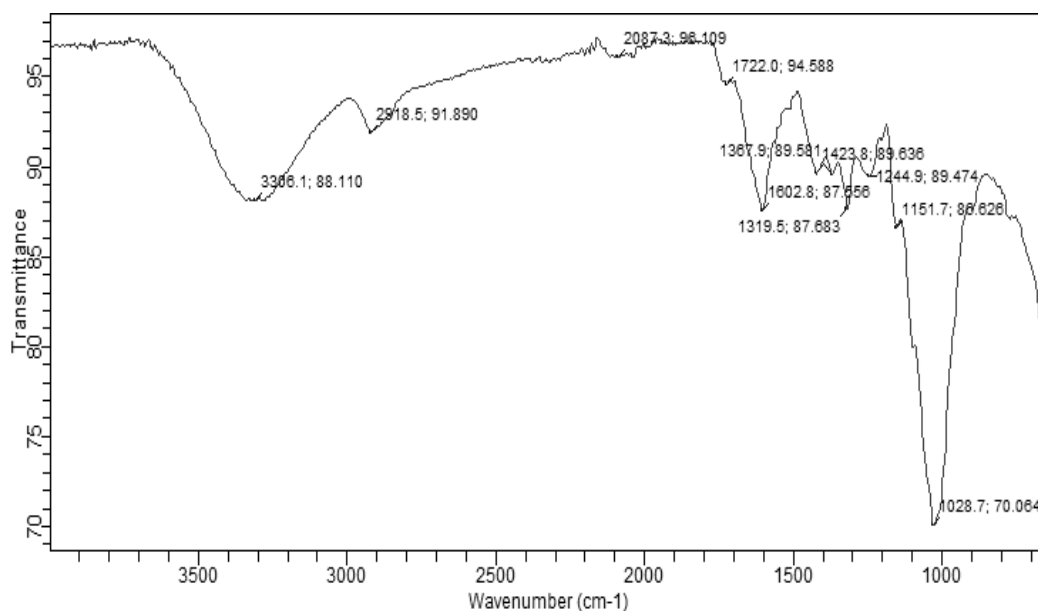


Figure 7: FTIR of Water Hyacinth Fibre

DISCUSSIONS

Physical and Chemical Characterization

The results of the physio-chemical characteristics of water hyacinth plant fibre shows that water hyacinth fibre has properties which are of interest. The average of the diameter of the WHF, measured at three (3) positions of the fibre as shown in Table 1 is approximately 229.5 μm . The moisture content is approximately 13.7 %, density of 666.7 kgm^{-3} , specific gravity 0.86, and water absorption 1067 % (Table 2). Similar results on the densities of grass, dry and apparent wet or compact, using toluene displacement method have been given as $1421 \pm 16 \text{ kgm}^{-3}$, and $1023 \pm 28 \text{ kgm}^{-3}$, respectively [36].

The cellulose, hemicellulose, lignin, ash, crude protein, and fibre are given as 14.1, 21.5, 7.1, 10.9, 3.9, and 29.1 % (Table 3), respectively. Cellulose determines the tensile strength of the material; lignin is responsible for resistance against biodegradation; and hemicellulose binds the cellulose polymers, provides secondary strength, and absorbs moisture [7]. A comparison of past results on the percentage cellulose, hemicellulose and lignin with the present research is shown in Table 4. The percentages of cellulose, hemicellulose and lignin recorded in this research are different from those achieved by previous researchers. The variabilities in composition have been attributed to environmental factors which are dependent on where the WH plants are grown and harvested. Generally, from Table 4, it can be concluded that water hyacinth has a high carbohydrate and low lignin content [4]. The XRF Spectroscopy of the WHF showing the various metal mineral elements in the WHF plant are shown in Table 5. It shows that the WHF is composed of seventeen (17) elements of various concentrations as follows: Ca, Na, K, Mn, Cu, Zn, Fe, Ni, Al, S, Mg, Rb, Sr, Br, Cl, Cr and V. These elements are what gives the WHF the peculiar characteristics in its performances. Ibrahim et al [37] XRF results on WH are compared with the present values achieved. The results show variabilities. This confirms that the environmental factors, and where the WH is taken, have tremendous effect on the characteristics of the fibre. It is therefore important to have arrays of data on WH fibre and their characteristics. This will impact greatly in the use of natural fibre as reinforcement material.

Mechanical Characterization of Water Hyacinth Fibre

Tensile Strength of WHF

Tables 6 and Figure 2 are the mechanical and statistical characteristics of the WHF. and the stress-strain of the WHF. Table 6 shows that the tensile strength is 0.12 MPa, young modulus, 7.7 GPa, elongation 4.8 %, and

tensile extension at break, 2.89 mm, and energy at break is 1.04×10^{-3} J. Similar values for the tensile strength and elongation of WHF fibre are given as 212gf/2.5 % [38] and 109.54 gf/den/6.65 % [39], respectively. The differences in elongation are an increase of approximately 48 % and a decrease of 35 %, respectively, for the two (2) WH fibres referenced. Natural cellulose includes crystalline and amorphous regions. Cellulose content and cellulose crystallinity are two critical microstructural parameters that affect the fibre tensile properties such as tensile strength (TS), Young's modulus, elongation at break and plastic shrinkage [40] Water hyacinth fibres are materials in which the covalent bond dominates. The rate of this type of bond is quantified by the crystallinity, and therefore, its high value reduces the degree of freedom for the molecular chains to move, thus ensuring the fibre strength.

Structural Characteristics of Water Hyacinth Fibre

XRD Analysis of the WHF

Figure 4 shows the XRD diffractogram of the WHF and their peaks. While cellulose does not occur as an individual molecule it is composed of crystalline and amorphous components. From the diffractogram there is no visible peak, showing crystal cellulose but suggests that it contains both amorphous and crystalline cellulose with visible peaks at $2\theta = 26.9^\circ$ to 27.4° . Amorphous cellulose occurs at lower 2θ such as 16° to 18° , while crystalline cellulose showed a peak at higher degrees such as 22.6° as suggested by Mukaratirwa et al. [41].

Thermographic characteristics

The TGA/DTG graphs (Figure 5 (a-c)) show decomposition of samples with respect to temperature. There are three (3) distinct stages of decomposition in the thermal degradation of WH fibre. The weight loss (TGA) and DTA peak in the first stage can be attributed to water loss [42]. The weight loss of 15 wt. % was recorded from 40-140 °C. The thermal degradation of the main lignocellulosic constituents of the fibre begins to occur at the onset of the second stage. A noticeable shoulder was observed from 221-346 °C with corresponding weight loss of 48 wt. %. The third stage is the decomposition of cellulose; the shoulder peak to the hemicellulose and the tail peak to the end of the lignin decomposition. A visible short shoulder is further observed at 350-426 °C, which represents the cellulose decomposition accounting for about 9.0 wt. %. It has been confirmed that lignocellulosic fibres are sensitive to temperature, and complete thermal degradation is expected above 400 °C [43,44]. Hemicellulose thermal degradation occurs before cellulose. The later weight loss recorded between 450-700 °C represent residual lignin decomposition which account for 4.5 wt%. The degradation of lignin occurs in a broader range that initiates earlier but extends to higher temperatures than those of hemicellulose and cellulose degradation [45]. From the DTG curve (Figure 5), the peak is identified at around 300 °C. This could be due to cellulose early and late degradation of cellulose. The peak at around 300 °C is due alignment of degradation profile of hemicellulose with some component of cellulose. while the later is pure cellulose decomposition profile. This exhibited reaction intensities of 1.2 and 3.7 wt. %/°C corresponding to early and late cellulose decomposition reaction. Hemicellulose is found to decompose at a maximum of 290 °C and up to 150 kJ/mol for activation energy, while lignin would thermally decompose with peaks from 280 to 520 °C and up to 229 kJ/mol for activation energy [46].

Morphology and Structural Characteristics of Water Hyacinth Fibre

Morphological Characteristics of Water Hyacinth Fibre

The morphological characteristics and element composition of the WHF are shown in Figure 6 and Table 7. The WH fibre has well-shaped fibril with rigid lignin structure coated surface, and the hollow space shows the fibre has the capacity to hold the liquid contents and and that the fibre has good absorbency [38]. A firm and highly ordered structure in WH biomass using SEM was also reported by Thi et al [47]. Tables 7 shows WH fibre contains calcium (Ca), sodium (Na), potassium (K), silver (Ag), silicon (Si), chlorine (Cl), zinc (Zn), ferrum (Fe), carbon (C), Sulphur (S), strontium (Sr), aluminum (Al), magnesium (Mg), phosphorous

(P), oxygen (O), nitrogen (N), yttrium (Y), and titanium (Ti) in various proportions. For weight (%) greater than 12 %, Table 7 shows four (4) dominant elements, and these are Ca, K, Cl, and C. This behaviour is comparable to results of previous research on WH as shown in Table 8 [34]. However, comparing [34] with [35], oxygen is not detected, both with the present work and the results on TR and YL. This points to the intrinsic variabilities in their properties ranging from age of the plant and its harvesting time to soil fertility and weather variations as mentioned by Claudia et. Al. [2].

FTIR of Water Hyacinth Fibre

FT-IR analysis allows determining the specific IR peaks relating to the cellulose crystallinity of the fibre as well as the qualitative difference of the main constituent elements of the fibre such as cellulose (amorphous or crystalline), hemicellulose and lignin. These elements have atomic bonds proper to their respective structure and an IR peak obtained by FT-IR gives information on the existence of these bonds. Given that the cellulose crystallinity is an intrinsic property which affects fibre strength, the evaluation of this cellulose crystallinity would help in the determination of the fibre tensile strength. The absorption bands for characteristic chemical groups of the lignocellulose *WH* fibre can be observed in Figure 8.

Figure 7 shows the specific absorption of the functional groups in the cellulose at wavenumber 3366.1 cm^{-1} which is the stretching vibration of the hydroxyl group (-OH). At wavenumber 2918.5 cm^{-1} shows stretching vibration of -CH₂ group. The emergence of -OH and -CH₂ group are groups found in the structure of cellulose. At wavenumber of 1028.7 cm^{-1} is the stretching vibration of the C-O group, which is the connecting group of the carbon chain in the cellulose structure, or it's called a glycoside bonding. The peak at 1319.5 cm^{-1} is a stretching vibration of -OH. In addition, the FT-IR spectrum shows the absorption of the lignin functional group in the C=O and C=C groups at wavenumbers 1423.8 cm^{-1} and 1244.9 cm^{-1} , respectively. The IR spectrum peaks used to determine crystallinity are 3200, 2200, 1722, 1680, 1280 and 860 cm^{-1} [9, 37] (Figure 7). The TCI and LOI indices defined as the total crystallinity index, and the lateral order index, respectively, are used to evaluate the IR crystallinity ratio. The HBI, which is the hydrogen bond intensity, is used to evaluate the hydrogen bond intensity of cellulose. This ratio is closely related to the crystal system and the degree of intermolecular regularity, that is, crystallinity, as well as the amount of bound water) [33]. The LOI, TCI and HBI are given as 1.49, 0.58 and 2.51, respectively.

CONCLUSION

The biological, chemical, and structural characterizations of water hyacinth plant fibre have been presented and the conclusions on the findings are as follows:

I- The WH plant fibre has a moisture content of approximately 13.7 %, density of 666.7 kg/m^3 , specific gravity of 0.86, and water absorption of 1067 %. The cellulose, hemicellulose, lignin, ash, crude protein, and fibre are given as 14.1, 21.5, 7.1, 10.9, 3.9, and 29.1 %, respectively. The variabilities in composition have been attributed to environmental factors which are dependent on where the WH plants are grown and harvested. Therefore, the fibre has good absorbency, less lignin content and high density.

II-The various metal mineral elements in the WHF plant detected using the XRF spectroscopy are Mo, Zr, Sr, Rb, Pb, As, Zn, Fe, Mn, Ti, Sc, Ca, K, S, Ba, and Nb, in various concentrations, and the mechanical strength together with the stress-strain of the WHF show WH fibre has a tensile strength of 0.12 MPa, young modulus, 7.7 GPa, elongation 4.8 %, tensile extension at break, 2.89 mm, and energy at break is 1.04×10^{-3} J, respectively.

III- The morphology of WH fibre shows a well-shaped fibril with a rigid lignin structure coated surface with the capacity to hold the liquid contents with good absorbency. The chemical compound compositions of the WH fibre contains Ca, K, Cl, C, Al, Si, Fe, S, Y, Ti, P, Mg, Na, and N.

IV-The XRD diffractogram characterization shows that the WH fibre is crystalline in nature, while the FT-IR

shows the functional group change of each treatment respectively. The thermal decomposition process of the WH fibre resulted in similar TG and DTG curves due to being lignin cellulosic material. These curves showed a distinct DTG peak (cellulose) and a high-temperature tail (lignin).

REFERENCE

1. Viola Hospodarova, Eva Singovszka, Nadezda Stevulova (2018). "Characterization of cellulosic fibres by FTIR Spectroscopy for their further implementation to building materials." *American Journal of Analytical Chemistry*, 9, 303-310. <https://doi.org/10.4236/ajac.2018.9602>.
2. Cláudia I. T. Navarro, Sidnei Paciornik, and José R. M. d'Almeida (2013). "Microstructural Characterization of Natural Fibers: Etlingera elatior, Costus comosus, and Heliconia bihai." *Hindawi Publishing Corporation Conference Papers in Materials Science Volume 2013*, Article ID 878014, 7 pages <http://dx.doi.org/10.1155/2013/87801>
3. Adela Salas-Ruiz 1, María del Mar Barbero-Barrera 1 and Trinidad Ruiz-Téllez (2019). "Microstructural and thermo-physical characterization of a Water Hyacinth petiole for thermal insulation particle board manufacture." *Materials*, 12, 560; doi:10.3390/ma12040560
4. Biswanath Biswas, Ajit Kumar Banik, Asit Baran Biswas (2015). "Comparative study of various pre-treatment techniques for saccharifications of water hyacinth (*eichhornia crassipes*) cellulose." *International Journal of Biotech Trends and Technology (IJBT)* - 5 (3): 11-16.
5. Asyraf, M.R.M.; Rafifidah, M.; Azrina, A.; Razman, M.R. Dynamic mechanical behaviour of kenaf cellulosic fibre biocomposites: A comprehensive review on chemical treatments. *Cellulose* **2021**, *28*, 2675–2695. [CrossRef]
6. Gowthaman, S.; Nakashima, K.; Kawasaki, S. A state-of-the-art review on soil reinforcement technology using natural plant fibre materials: Past findings, present trends and future directions. *Materials* **2018**, *11*, 553. [CrossRef] [PubMed]
7. Bordoloi, S.; Kashyap, V.; Garg, A.; Sreedeeep, S.; Wei, L.; Andriyas, S. Measurement of mechanical characteristics of fibre from a novel invasive weed: A comprehensive comparison with fibres from agricultural crops. *Measurement* **2018**, *113*, 62–70. [CrossRef]
8. Abrial, H.; Dalimunthe, M.H.; Hartono, J.; Efendi, R.P.; Asrofi, M.; Sugiarti, E.; Sapuan, S.M.; Park, J.W.; Kim, H.J. Characterization of tapioca starch biopolymer composites reinforced with micro scale water hyacinth fibers. *Starch-Stärke* **2018**. [CrossRef]
9. Komuraiah, A.; Kumar, N.S.; Prasad, B.D. Chemical composition of natural fibers and its influence on their mechanical properties. *Mech. Compos. Mater.* **2014**, *50*, 359–376. [CrossRef]
10. ASTM D2495 (2007). Standard Test Method for Moisture in Cotton by Oven-Drying
11. Syed Abd Aziz, Sharifah Hanisah, Raja hedar, Raja Jamal, and Abdullah, Zahid. *The determination of bulk (apparent) density of plant fibres by density method*. Malaysia: N. p., 2004. Web.
12. ASTM D570 (2018). Standard Test Method for Water Absorption of Plastics
13. AOAC (Association of Official Analytical Chemists) (1995) Official methods of analysis, 16th Ed. Association of Official Analytical C Washington DC, USA
14. TAPPI T264 cm-97 (20000a) "Preparation of wood for chemical analysis." TAPPI Press, Atlanta, GA.
15. Opeyemi, I. Ayanda, Tolulope, Ajayi; Femi P. Asuwaja (2020). "Eichhornia Grassipes (Mart.) Solms: Challenges, treats. And prospects." *Hindawi, The Scientific World Journal*. Article ID3452172, 12 pages. <https://>
16. R. Kumar, G. Mago, V. Balan, and C.E. Wyman (2009). "Physical and chemical characterization of corn stover and poplar solids resulting from loading pretreatment technologies." *BioResource Technology*, *100* (17): 3948-3962.
17. Sornvoraweat and J. Kongkiattikajorn (2010). "Separated hydrolysis and fermentation of water hyacinth leaves for ethanol production." *Asia Pacific Journal of Science and Technology*, *15* (9): 794-802.
18. Rezanian, H. Alizadeh, J. Cho, N. Darajeh, J. Park, B. Hastemi, M.F.M. Din, S. Krishnan, K.K. Yadar, N. Gupta and S. Kumar (2019). "Changes in composition and structure of water hyacinth based on various pretreatment methods." *BioResources*, *14* (3): 6088-6099.

19. M; Narra, J. Divecha, D. Shah, V. Balasubramanian, B. Vyas, M. Harijan, and K. Macuan (2013). "Cellulase production, simultaneous saccharification and structure and biogas production of water hyacinth (*Eichhornia crassipes*)." *BioResource Technology*, 132: 361-364.
20. B. Barua and A.S. Kalamdhad (2017). "Effect of various types of thermal pretreatment techniques on the hydrolysis, compositional analysis and characterization of water hyacinth." *Bioresource Technology*, 227: 147-154
21. Rezania, H. Alizadeh, J. Cho, N. Darajeh, J. Park, B. Hastemi, M.F.M. Din, S. Krishnan, K.K. Yadar, N. Gupta and S. Kumar (2019). "Changes in composition and structure of water hyacinth based on various pretreatment methods." *BioResources*, 14 (3): 6088-6099.
22. . Kumari and D. Das (2019). "Biohythane production from sugarcane bagasse and water hyacinth: A way towards promising green energy production." *Journal of Cleaner Production*, 207: 689-701.
23. Mochomadd Asrofi, Hairal Abral, Anwar Kasim, Acyar Pratoto, Melbi Machardiba and Fadli Hafizulhaq (). "Mechanical properties of water hyacinth nanofibre cellulose reinforced thermoplastic starch bionanocomposite: Effect of ultrasonic vibration during processing." *Natural Fibre Biocomposites*, Edited by Prof. Sheldon Shlilyio,
24. Auanga Boontum, Jirapa Phetsan, Wawat Rodiahwati, Kanyarat Kitsubthawee, Teerachai Kuntothom (2019). "Characterization of diluted-acid pretreatment of water hyacinth." *Applied Science and Engineering Progress*, 12 (4): 253-263.
25. Biswanta Biwas, Ajit Kumar Banik, Asit Baran Biswas (2015). "Comparative study of various pretreatment techniques for saccharifications of water hyacinth (*Eichhornia crassipes*) cellulose." *Int. J. of Biotech Trends & Technology (IJBTT)*, 5 (3): 11-16.
26. Bhuvaneshwavi and Dr. K. Sangeetha (2016). "Investigation of physical, chemical and structural characterization of *Eichhornia Crassipes* fibre." *Int. Conference on Information Engineering, Management and Security (ICIEMS)*, 92-96.
27. Winowlin Japps Jebas Thangiah, Ajithram Arivendan, Adaukhan Mahaoob Basha, Rajini Nagarajan, Reena Daphne (). "Serious environmental threat water hyacinth (*Eichhornia Crassipes*) plant natural fibres: Different extraction methods and morphological properties for polymer composite application." *Research Square*, 1-15.
28. Ajithram Arivendan, Winowlin Jappes, Jepas Thangiah, Siva Irulappasamy and Brintha N. Chrish (2022). "Study on characterization of water hyacinth (*Eichhornia Crassipes*) novel natural fibre as reinforcement with epoxy polymer matrix material for lightweight applications." *Journal of Industrial Textiles* 51 (5S): 8157S-8174S.
29. Fiiitoyaa Fitrya, Najiana A. Fithri, Dina P, Ngaya, Egi P. Senbiring (2012). "Optimization of acid concentration and hydrolysis time in the isolation of microcrystalline cellulose from water hyacinth (*Eichhornia Crassipes* Slom." *Special Issue*.
30. AOAC (1990). "Official methods of analysis." *Association of Official Analytical Chemists*, Vol. I, 15th
31. ASTM D3822/D3822M-14. Standard Test Method for Tensile Properties of Single Textile Fibers
32. M. Nurazzi, M. R. M. Asyraf, M. Rayung, M. N. F. Norrahim, S. S. Shazleen, M. S. A. Rani, A. R. Shafi, H. A. Aisyah, M. H. M. Radzi, F. A. Sabaruddin, R. A. Ilyas, E. S. Zainudin, and K. Abdan (2021). "Thermogravimetric Analysis Properties of Cellulosic Natural Fiber Polymer Composites: A Review on Influence of Chemical Treatments. *Polymers*", 13, 2710. <https://doi.org/10.3390/polym13162710>.
33. A Ajithram, JT Winowlin Jappes, M Adam khan and NC Brintha (). "Evaluation of mechanical properties and thermal characteristics of aquatic wastewater hyacinth (*Eichhornia crassipes*) plant into natural powder and ash reinforced polymer composites for lightweight applications. *J Mechanical Engineering Science* 0 (0) 1–12. DOI: 10.1177/09544062211038982
34. S Lara-Serrano, O.M. Rutiago-Quiñones, J. López-Mirinda, H.A Fileto-Pérez, F.E. Pedraza-Bucio, J.L. Rico-Cerda, and J.G. Rutiaga- Quiñones (2016). "Physicochemical characterization of water hyacinth (*Eihornia crassipes* (Mart.) Solms). "Water Hyacinth", *BioResources* 11 (3): 7214-7223.
35. Sukarni Sukarni, Yahya Zakaria, Sumarli Sumarli, Retno Wulandari, Avita Ayu Permanasari, M. Suhermanto (2019). "Physical and Chemical Properties of Water Hyacinth (*Eichhornia crassipes*) as a

- Sustainable Biofuel Feedstock.” *Materials Science and Engineering* 515 012070 doi:10.1088/1757-899X/515/1/012070.
36. B. McNulty and S. Kennedy (1982). “Density measurements of grass by toluene displacement and air comparison pycnometry.” *Irish Journal of Agricultural and Food Research*, 21:75-83.
 37. 21-Medhat Ibrahim, Ragab Mahan, Osama Osman and Traugott Scheytt (2010). “Effect of Physical and Chemical Treatments on the Electrical and Structural Properties of Water Hyacinth.” *The Open Spectroscopy Journal*, 4, 32-40
 38. M Bhuvaneshwari, Dr K Sangeetha (2016). “Investigation of physical, chemical and structural characterization of Eichhornia crassipes fibre”. *International Conference on Information Engineering, Management and Security*: 92-96. Print.
 39. Sakorn Chonsakorn, Supanicha Srivorradatpaisan & Rattanaphol Mongkholrattanasit (2019) “Effects of different extraction methods on some properties of water hyacinth fibre”, *Journal of Natural Fibres*, 16:7, 1015-1025, DOI: 10.1080/15440478.2018.1448 316
 40. H. Rafidson, H. Ramaswamy, J. Chummun, F.B.V. Florens (2020). “Using infrared spectrum analyses to predict tensile strength of fibres in a group of closely related plant species: case of Mascarenes Pandanus spp. *SN Applied Sciences* 2:1922|<https://doi.org/10.1007/s42452-020-03667-1>
 41. Netai Mukaratirwa-Muchanyereyi, Jameson Kugara and Mark Fungayi Zaranyika (2016). “Surface composition and surface properties of water hyacinth (*Eichhornia crassipes*) root biomass: Effect of mineral acid and organic solvent treatment.” *African Journal of Biotechnology*, 15 (21), 897-909, DOI: 10.5897/AJB2015.15068.
 42. Rani, M.S.A.; Mohammad, M.; Sua’it, M.S.; Ahmad, A.; Mohamed, N.S (2020). “Novel approach for the utilization of ionic liquid-based cellulose derivative biosourced polymer electrolytes in safe sodium-ion batteries”. *Bull.* 78, 5355–5377. [CrossRef]
 43. Monteiro, S.N.; Calado, V.; Rodriguez, R.J.S.; Margem, F.M (2012). “Thermogravimetric behavior of natural fibers reinforced polymer composites-An overview.” *Sci. Eng. A*, 557, 17–28. [CrossRef]
 44. Yang, H.; Yan, R.; Chen, H.; Lee, D.H.; Zheng, C (2007). “Characteristics of hemicellulose, cellulose and lignin pyrolysis.” *Fuel*, 86, 1781–1788. [CrossRef]
 45. Mészáros, E.; Jakab, E.; Várhegyi, G (2007). TG/MS, Py-GC/MS and THM-GC/MS study of the composition and thermal behavior of extractive components of *Robinia pseudo acacia*. *Anal. Appl. Pyrolysis*, 79, 61–70. [CrossRef]
 46. Nguyen, T.; Zavarin, E.; Barrall, E.M (1981). “Thermal Analysis Of Lignocellulosic Materials.” Part II. Modified Materials. *Macromol. Sci. Part C*, 20, 1–65. [CrossRef]
 47. Thi, BTH, Ong, IK., Thi, DTN, and Ju, YH (2017). “Effect of subcritical water pretreatment on cellulose recovery of water hyacinth (*Eichhornia crassipes*)”. *Journal of the Taiwan Institute of Chemical Engineers* 71 ©, 55-61. DOI: 10.1016/j.jtice 2016.12.028.